Feasibility of imaging of epidermal growth factor receptor expression with ZEGFR:2377 affibody molecule labeled with ^{99m}Tc using a peptide-based cysteine-containing chelator

KEN G. ANDERSSON[1*], MARYAM OROUJENI[2*], JAVAD GAROUSI[2], BOGDAN MITRAN[3], STEFAN STÅHL[1], ANNA ORLOVA[3], JOHN LÖFBLOM[1] and VLADIMIR TOLMACHEV[2]

[1]Division of Protein Technology, KTH Royal Institute of Technology, SE-10691 Stockholm;
[2]Institute of Immunology, Genetic and Pathology, Uppsala University, SE-75185 Uppsala;
[3]Division of Molecular Imaging, Department of Medicinal Chemistry, Uppsala University, SE-75183 Uppsala, Sweden

Received June 27, 2016; Accepted August 30, 2016

DOI: 10.3892/ijo.2016.3721

Abstract. The epidermal growth factor receptor (EGFR) is overexpressed in a number of malignant tumors and is a molecular target for several specific anticancer antibodies and tyrosine kinase inhibitors. The overexpression of EGFR is a predictive biomarker for response to several therapy regimens. Radionuclide molecular imaging might enable detection of EGFR overexpression by a non-invasive procedure and could be used repeatedly. Affibody molecules are engineered scaffold proteins, which could be selected to have a high affinity and selectivity to predetermined targets. The anti-EGFR ZEGFR:2377 affibody molecule is a potential imaging probe for EGFR detection. The use of the generator-produced radionuclide ^{99m}Tc should facilitate clinical translation of an imaging probe due to its low price, availability and favorable dosimetry of the radionuclide. In the present study, we evaluated feasibility of ZEGFR:2377 labeling with ^{99m}Tc using a peptide-based cysteine-containing chelator expressed at the C-terminus of ZEGFR:2377. The label was stable *in vitro* under cysteine challenge. In addition, ^{99m}Tc-ZEGFR:2377 was capable of specific binding to EGFR-expressing cells with high affinity (274 pM). Studies in BALB/C nu/nu mice bearing A431 xenografts demonstrated that ^{99m}Tc-ZEGFR:2377 accumulates in tumors in an EGFR-specific manner. The tumor uptake values were 3.6±1 and 2.5±0.4% ID/g at 3 and 24 h after injection, respectively. The corresponding tumor-to-blood ratios were 1.8±0.4 and 8±3. The xenografts were clearly visualized at both time-points. This study demonstrated the potential of ^{99m}Tc-labeled ZEGFR:2377 for imaging of EGFR *in vivo*.

Correspondence to: Professor Vladimir Tolmachev, Institute of Immunology, Genetic and Pathology, Uppsala University, Dag Hammarskjölds väg 20, SE-75185 Uppsala, Sweden
E-mail: vladimir.tolmachev@igp.uu.se

*Contributed equally

Abbreviations: EGFR, epidermal growth factor receptor; RTK, receptor tyrosine kinase; HNSCC, head and neck squamous cell carcinoma; NSCLC, non-small cell lung cancer; TKI, tyrosine kinase inhibitor; SPECT, single photon emission computed tomography; PBS, phosphate-buffered saline; DTT, dithiothreitol; SDS-PAGE, sodium dodecyl sulfate polyacrylamide gel electrophoresis; HPLC, high performance liquid chromatography; RHT, reduced hydrolyzed technetium; K_D, equilibrium dissociation constant; PET, positron emission tomography

Keywords: epidermal growth factor receptor, radionuclide molecular imaging, affibody molecules, technetium-99m, A431, biodistribution

Introduction

Visualization of alterations in cell-surface receptor expression in malignant cells may identify molecular targets enabling specific treatment of an individual tumor. A spectacular example of such an approach is the clinical use of imaging of the expression of somatostatin receptors for patient selection for subsequent therapy using radiolabeled somatostatin analogues (1). Relatively recently, *in vivo* imaging of receptor tyrosine kinase (RTK) expression has attracted increased attention (2,3). RTKs normally regulate cellular division, differentiation, motility and apoptosis, i.e. phenomena that are essential in malignancies. Aberrant expression of RTKs is often one of the driving forces of a malignancy, and targeting of overexpressed RTKs is one of the major directions in development of anticancer drugs (4). The epidermal growth factor receptor (EGFR) is an RTK that is often overexpressed in a variety of malignancies (5). Overexpression/amplification of EGFR is associated with shorter survival in gastric and esophageal adenocarcinoma (6), pancreatic adenocarcinoma (7), vulvar carcinoma (8), head and neck squamous cell carcinoma (HNSCC) (9) and glioma (10). EGFR is a well-established target for monoclonal antibodies and specific tyrosine kinase inhibitors (11).

The specific character of anti-EGFR therapeutics necessitates an identification of patients with tumors that will respond to therapy. The expression level of the receptor is one of the possible predictors for the response. In some cases, overex-

pression of EGFR cannot be a sole predicting biomarker. For example, presence of specific mutations in the kinase domain of EGFR is a precondition to response of non-small cell lung cancer (NSCLC) to the tyrosine kinase inhibitor gefitinib in a number of settings (12,13). Metastatic colorectal cancer would not respond to anti-EGFR antibody-treatment in the case of mutations in the intracellular signaling cascades (14). However, information concerning the expression level of wild-type EGFR is helpful in selection of the optimal treatment in many other instances. Non-small cell lung cancer overexpressing EGFR would be more likely to respond to the addition of cetuximab to a first-line chemotherapy (15) and to treatment with gefitinib (16,17) compared to NSCLCs with low EGFR expression. The addition of cetuximab to chemoradiotherapy of stage III HNSCC significantly improves survival of patients with tumors having high EGFR expression (18). In the case of low EGFR expression, the use of cetuximab shortens survival. In HNSCC, high expression of EGFR is associated with relapse after radiotherapy (19). For such patients, accelerated radiotherapy fractionation would provide advantages compared to conventional radiation treatment (20,21). High expression of EGFR in esophageal squamous cell carcinoma is a precondition for successful treatment with the TKI icotinib (22). High EGFR expression is a negative predicting biomarker for response of triple-negative breast cancer to neoadjuvant therapy using anthracyclines and taxanes (23). The main problem is that the expression level of EGFR can vary during the metastasis process, and the discordance rate between biopsy samples from primary NSCLC and metastases might be up to 50% (24). This necessitates a reliable methodology for assessment of EGFR expression in disseminated cancer.

The use of radionuclide molecular imaging has a potential for non-invasive estimation of EGFR expression in multiple metastatic sites. Several radiolabeled monoclonal anti-EGFR antibodies have been evaluated as imaging probes (25-28). The feasibility of *in vivo* imaging of EGFR expression has been demonstrated in these studies. However, all radiolabeled antibodies clear slowly from blood and non-specific compartments, which results in moderate contrast and requires several days between injection of the antibody and imaging. The use of smaller radiolabeled fragments of cetuximab as imaging agents increased appreciably the contrast of EGFR imaging and enabled shortening of the time between injection of the probe and the imaging session (29,30). A smaller size of the $(Fab')_2$-fragment contributed to both more rapid clearance and better tumor localization, which demonstrated advantages of a reduction of the imaging probe size for improved contrast. An alternative to the use of monoclonal antibodies for imaging of EGFR is the use of affibody molecules.

Affibody molecules are small affinity proteins that can be engineered to bind a large repertoire of different target proteins through creation of combinatorial libraries and a subsequent selection procedure for the isolation of target-specific binders (31). Combination of small size (6-7 kDa) with high affinity makes affibody molecules attractive as imaging probes, which has been shown in preclinical (32) and clinical studies (33). Several anti-EGFR affibody molecules have been developed and labeled with ^{111}In (34,35) for SPECT and ^{18}F (36,37) or ^{89}Zr (38) for PET imaging. The present study

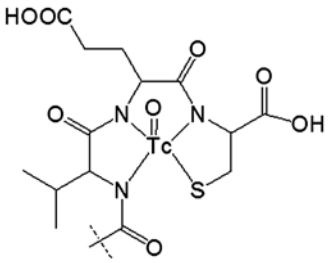

Figure 1. Structure of ^{99m}Tc complex with peptide-based cysteine-contained N_3S chelator at C-terminus.

was focused on the ZEGFR:2377 affibody molecule (35,39), which has equal affinity to human and murine EGFR. This feature is essential since EGFR is expressed in a number of normal tissues. The cross-reactivity with murine receptor makes mouse models adequate to study all aspects of *in vivo* targeting.

The rapid progress in the design and performance of SPECT cameras during the last years (40) suggests that the development of molecular imaging probes labeled with single-photon emitters remains to be of interest. The use of the generator-produced radionuclide ^{99m}Tc as a label would be preferable for this purpose, as this nuclide offers a number of advantages compared to alternative labels, such as ^{111}In or ^{123}I which includes low cost, excellent availability and favorable dosimetry (41).

We have reported earlier labeling of anti-HER2 affibody molecule ZHER2:2395 with ^{99m}Tc using incorporation of cysteine at C-terminus (42). The thiol group of cysteine forms together with amide nitrogen of adjacent amino acids a N_3S chelator providing a stable complex with ^{99m}Tc (42) (Fig. 1). Such approach might be considered for anti-EGFR affibody ZEGFR:2377 as well. However, our studies have demonstrated that modification of the amino acid sequence of affibody molecule might create an alternative binding site for technetium-99m, providing lower stability of the complex (43). Since the amino acid composition of ZEGFR:2377 differs profoundly from the composition of ZHER2:2395 we had to consider formation of an alternative chelating site as well.

The aim of the present study was to evaluate the feasibility of imaging of EGFR expression with the ZEGFR:2377 affibody molecule labeled with ^{99m}Tc using peptide-based cysteine-containing chelator.

Materials and methods

^{99m}Tc-pertechnetate was obtained by elution of a generator (Mallinckrodt-Tyco, Petten, The Netherlands) with sterile 0.9% sodium chloride. Radioactivity in cell and biodistribution studies was measured by an automated gamma-spectrometer (1480 Wizard; Wallac Oy, Turku, Finland). The Cyclone Storage Phosphor system (Perkin-Elmer, Wellesley, MA, USA) was used for quantitative measurement of radioactivity distribution in instant thin-layer chromatography strips and electrophoresis gels.

An unpaired t-test was used to determine if the difference between the measured values in the biological experiments was significant ($P<0.05$).

Preparation of ^{99m}Tc-ZEGFR:2377. The EGFR specific affibody molecule ZEGFR:2377 was produced as previously described (45). Briefly, the affibody molecule was recombinantly produced overnight at 25˚C in *E. coli* BL21 Star (DE3) (Thermo Fisher Scientific, Inc., Stockholm, Sweden) by induction with 100 μM IPTG at an OD600 of 0.6. The lysed cells were heat-shocked at 90˚C for 10 min and the affibody molecule was recovered using a Q-Sepharose column (GE-Healthcare, Uppsala, Sweden). A polishing step was done using RP-HPLC (Zorbax 300SB-C18; Agilent Technologies, Inc., Palo Alto, CA, USA). The purity was measured using RP-HPLC using a gradient from 20-60 for 25 min at a flow rate of 1 ml/min (A: 0.1% trifluoroacetic acid in water; B: 0.1% trifluoroacetic acid in acetonitrile). Determination of mass was done using electrospray on-line mass spectrometry (Agilent Technologies).

Before labeling, the ZEGFR:2377 affibody molecule was treated with dithiothreitol (DTT; Merck, Darmstadt, Germany) to reduce the disulphide bonds formed by cysteines. For this purpose, a solution of DTT (3.5 μl, 1 M in degassed 0.2 M sodium phosphate buffer, pH 8.0) was mixed with affibody molecules (100 μl, 5 mg/ml in 0.2 M sodium phosphate buffer, pH 8.0) to obtain a final DTT concentration 30 mM. The mixture was incubated at 40˚C for 90 min under argon atmosphere. Purification of reduced affibody molecules was performed using NAP-5 column equilibrated and eluted with PBS. The solution of the reduced affibody molecules was divided in aliquots, 100 μg in 180 μl PBS each and stored at -80˚C.

A freeze-dried labeling kit containing 75 mg of tin (II) chloride dihydrate (Fluka Chemika, Buchs, Switzerland), 5 mg of gluconic acid sodium salt (Celsus Laboratories, Geel, Belgium) and 100 μg of EDTA (Sigma-Aldrich, Munich, Germany) was prepared for labeling of affibody molecules with ^{99m}Tc as describe earlier (44).

For a typical labeling, 50 μg of the reduced ZEGFR:2377 in PBS (90 μl), was mixed with one freeze-dried kit and 100 μl of ^{99m}Tc-pertechnetate generator eluate (typically, 500-800 MBq) was added. The mixture was incubated at 90˚C for 60 min. To remove loosly affibody-bound ^{99m}Tc, a treatment with excess of cysteine was used. A fresh solution of cysteine (1 mg/ml in PBS, 300-fold molar excess to affibody molecules, was added to the labeled conjugate and incubated at 90˚C for 15 min. After challenge, ^{99m}Tc-ZEGFR:2377 was isolated using size-exclusion chromatography on disposable NAP-5 columns, pre-equilibrated and eluted with PBS.

Labeling yield and purity of affibody molecules were analyzed using ITLC-SG (Agilent Technologies) developed with PBS (affibody: Rf=0.0; other forms of ^{99m}Tc: Rf=1.0). The reduced hydrolyzed technetium colloid (RHT) level in the product was measured using pyridine:acetic acid:water (5:3:1.5) as the mobile phase (^{99m}Tc colloid: Rf=0.0, other forms of ^{99m}Tc and radiolabeled affibody molecule: Rf=1.0). The results of the ITLC measurement were validated by a sodium dodecyl sulfate polyacrylamide gel electrophoresis (SDS-PAGE). This was performed using NuPAGE 4-12% Bis-Tris Gel in MES buffer (both from Invitrogen AB, Stockholm, Sweden) at 200 V constant during 30 min.

In vitro stability was evaluated using cysteine challenge (45). Samples of ^{99m}Tc-ZEGFR:2377 (5.6 μg, 50 μl) after purification were mixed with cysteine (5.2 μg, 1 mg/ml in PBS) to obtain a 300-fold molar excess of cysteine. Control samples were mixed with equal volume of PBS. In addition, a separate set of affibody samples was mixed with sodium ascorbate (13 μg, 1 mg/ml in PBS). The samples were incubated at 37˚C. At 1, 2 and 4 h after mixing, the radiochemical purity was determined by radio-ITLC as describe above. The experiment was performed in triplicate.

In vitro studies. The three different EGFR-expressing cell lines A431, MDA468 and PC3 (ATCC; purchased via LGC Promochem, Borås, Sweden), were used in the present study. The cell lines were cultured in McCoy's medium, supplemented with 10% fetal bovine serum (Sigma-Aldrich), 1% L-glutamine, and PEST (penicillin 100 U/ml and 100 μg/ml streptomycin), all from Bookroom AG (Berlin, Germany). The cells were cultured at 37˚C in a humidified incubator with 5% CO_2.

Binding specificity of the labeled affibody molecules was tested using cell lines with three different levels of EGFR expression (A431, MDA468 and PC3). Cells were seeded to three sets of dishes, ~10^6 cells/dish, and incubated for 1 h at 37˚C with 10 nM ^{99m}Tc-ZEGFR:2377. To two sets of control dishes, a 50-fold molar excess of either non-labeled ZEGFR:2377 or cetuximab was added before adding ^{99m}Tc-ZEGFR:2377. After incubation, the medium was aspired; the cells were washed with medium, detached using trypsin and collected. Radioactivity of cells was measured, and percentage of cell-bound radioactivity was calculated. The experiments were performed in triplicate.

To measure the affinity of the conjugate to EGFR, kinetics of binding of ^{99m}Tc-ZEGFR:2377 to and its dissociation from A431 cells were measured using a LigandTracer Yellow instrument (Ridgeview Instruments AB, Vänge, Sweden). The measurements were performed at room temperature to prevent internalization. Uptake curves were recorded at 0.33, 1 and 3 nM of ^{99m}Tc-ZEGFR:2377, thereafter the radioactive medium was withdrawn, fresh non-radioactive medium was added and the dissociation curve was recorded. The data were analyzed using the Interaction Map software (Ridgeview Diagnostics AB, Uppsala, Sweden) to calculate association rate, dissociation rate and dissociation constant at equilibrium (K_D).

Cellular processing of bound ^{99m}Tc-ZEGFR:2377 was evaluated using MDA486 and A432 cells. The cells were incubated with 10 nM ^{99m}Tc-ZEGFR:2377 at 37˚C. At 1, 2, 4, 6 and 24 h after incubation start, the internalized fraction was determined by an acid wash method adapted and validated for affibody molecules by Wållberg and Orlova (46). The membrane-bound affibody molecules were removed from cells by treatment with 4 M urea solution in a 0.1 M glycine buffer, pH 2.5, for 5 min on ice. The cell debris containing the internalized conjugates was detached by treatment with 1 M NaOH. Radioactivity of cells was measured, and percentage of membrane-bound and internalized radioactivity was calculated. The experiments were performed in triplicate.

In vivo studies. All applicable international, Swedish national and Uppsala University guidelines for the care and the use of the animals were followed. All procedures performed in studies involving animals were in accordance with the ethical

Table I. *In vitro* stability of ^{99m}Tc-ZEGFR:2377.

	Affibody-bound radioactivity, %				
	No cysteine challenge before purification		Cysteine challenge before purification		
	PBS	300-fold cysteine excess	PBS	300-fold cysteine excess	Sodium ascorbate
1 h	60.0±0.4	66±2	96±3	98±1	99.6±0.1
2 h	60.7±0.4	65.3±0.1	95±4	96±2	99.4±0.2
4 h	62.6±0.8	63±4	92±3	95.3±0.7	99±1

standards of the Uppsala University. The studies were approved by the Ethics Committee for Animal Research in Uppsala. Female BALB/C nu/nu mice were purchased from Taconic M&B a/S (Ry, Denmark). EGFR-expressing xenografts were established by subcutaneous injection of 10^7 A431 cells in the right hind legs of mice. The experiments were performed 12-14 days after tumor implantation. The average animal weight at the time of experiment was 19±2 g. The average tumor weight was 550±240 mg.

For biodistribution measurements, mice were randomly divided into groups of four animals each. To investigate the specificity of conjugate *in vivo*, EGF receptors were saturated in a control group of mice by subcutaneous injection of 2.5 mg of cetuximab 48 and 24 h before labeled conjugate injection. Two groups of mice (including control group) were intravenously injected with ^{99m}Tc-ZEGFR:2377 (60 kBq in 100 μl PBS per mouse) for biodistribution measurement at 3 h after injection. One group of mice was injected with 480 kBq for measurement of biodistribution at 24 h after injection. The injected protein dose was adjusted to 38 μg per mouse. This protein dose has been found to be optimal for imaging using ^{111}In-DOTA-ZEGFR:2377 in earlier studies (35).

The mice were euthanized at 3 and 24 h pi by overdosing of anesthesia. Blood, salivary glands, thyroid, lung, liver, spleen, colon, kidney, tumor, muscle and bone were collected in weighed plastic bottles. The radioactivity was measured and uptake was calculated as percent injected dose per gram tissue (%ID/g).

microSPECT/CT imaging of EGFR-expressing xenografts using ^{99m}Tc-ZEGFR:2377. BALB/C nu/nu mice bearing subcutaneous A431 xenografts were intravenously injected with 38 μg (30 MBq) ^{99m}Tc-ZEGFR:2377. Whole body scans were acquired using nanoScan SC (Mediso Medical Imaging Systems, Budapest, Hungary) at 3 and 24 h after injections. The mice were euthanized by CO_2 asphyxiation immediately before being placed on camera. The computed tomography (CT) acquisition was carried out at the following parameters: energy peak of 50 kV, 670 μA, 480 projections, 2.29-min acquisition time. SPECT acquisition was performed at the following parameters: ^{99m}Tc energy peak of 140 keV, window width of 20%, matrix of 256x256, acquisition time: 1 h. CT images were reconstructed in real-time using Nucline 2.03 Software (Mediso Medical Imaging Systems). SPECT raw data were reconstructed using Tera-Tomo™ 3D SPECT reconstruction technology. Coronal SPECT-CT images of the scans are presented as maximum intensity projections (MIP) in RGB color scale.

Results

Preparation of ^{99m}Tc-ZEGFR:2377. The anti-EGFR binding ZEGFR:2377 affibody molecule was produced and subsequently purified using heat-treatment of cells, anion exchange for product recovery and a reverse phase-HPLC polishing step. The purity of the protein was determined to 97.2% and the mass was resolved using mass-spectrometry to 14,781 Da (theoretical mass of dimer 14,782 Da and monomer 7,391 Da).

Initially, the labeling was performed according to protocol of Ahlgren and co-workers (44), i.e. without intermediate challenge before purification. The radiochemical yield was 99.6% and, after purification using NAP-5 column, radiochemical purity was 100%. However, the results of the *in vitro* stability test (Table I) demonstrated rapid release of ^{99m}Tc not only under cysteine challenge but also during storage in PBS.

There was a possibility that part of ^{99m}Tc was bound not to a cysteine-containing chelator, but to a much weaker chelating site. Therefore, we have introduced a cysteine challenge between labeling and chromatographic purification. The isolated yield of such procedure was 69.2±1.2%, and the purity of the conjugate after NAP-5 purification was 100±0%. The presence of RHT was 0.2±0.2% in all experiments. The maximum specific activity of 9 MBq/μg (66.5 GBq/μmol) was obtained.

The release of ^{99m}Tc under *in vitro* stability test was appreciably reduced, and >95% of radioactivity was associated with the affibody molecule after the 4-h cysteine challenge. Notably, there was higher release in the control than in cysteine challenge group. This indicated that a re-oxidation of ^{99m}Tc might play a role in its release. To test the hypothesis, we performed the stability test using sodium ascorbate as an antioxidant. The release of ^{99m}Tc has been appreciable reduced in this case (Table I). Sodium ascorbate has hence been included in formulation of ^{99m}Tc-ZEGFR:2377 for animal studies.

In vitro studies. The results of the *in vitro* specificity test of ^{99m}Tc-ZEGFR:2377 are presented in Fig. 2. Pre-saturation of EGFR with a large excess of both non-labeled ZEGFR:2377 and anti-EGFR antibody cetuximab reduced significantly ($P<0.0001$) binding of ^{99m}Tc-ZEGFR:2377 to EGFR-expressing cells. The saturable character of the binding suggests its specificity.

The LigandTracer measurements of the ^{99m}Tc-ZEGFR:2377 interaction with A431 cells showed a rapid binding (association rate of $2.77x10^5$ 1/M x sec) and slow dissociation (dissociation rate of $7.73x10^{-5}$ 1/sec). The dissociation constant (K_D) of ^{99m}Tc-ZEGFR:2377 interaction with A431 cells was 274 pM.

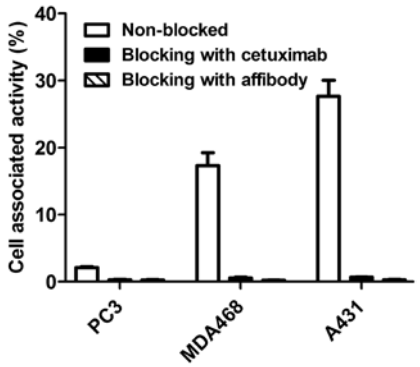

Figure 2. *In vitro* specificity of ^{99m}Tc-ZEGFR:2377 binding to three different EGFR-expressing cell lines. Cells were incubated with 10 nM ^{99m}Tc-ZEGFR:2377. A large molar excess of non-labeled ZEGFR:2377 or cetuximab was used for blocking of receptors. The data are presented as average (n=3-6) and SD.

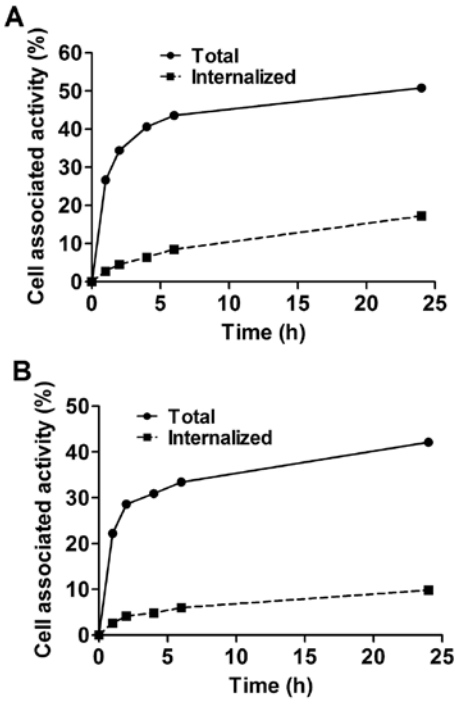

Figure 3. Cellular processing of ^{99m}Tc-ZEGFR:2377 by EGFR-expressing MDA468 (A) and A431(B) cell lines. Cells were incubated with 10 nM ^{99m}Tc-ZEGFR:2377. The data are presented as average (n=3) and SD. Error bars are not seen because they are smaller than point symbols.

The processing of bound ^{99m}Tc-ZEGFR:2377 by MDA468 and A431 cancer cell lines is presented in Fig. 3. The common feature for both cell lines was rapid binding and relatively slow internalization of ^{99m}Tc-ZEGFR:2377. Although the pattern of internalization was similar, the internalization by A431 cells was slower than by MDA468. The internalized fractions after 24-h incubation were 23.3±0.3 and 34.9±0.3% of total cell-bound radioactivity, for A431 and MD468, respectively.

In vivo studies. The specificity of ^{99m}Tc-ZEGFR:2377 binding to EGFR *in vivo* was demonstrated by *in vivo* saturation of receptors by injection of the monoclonal antibody cetuximab (Fig. 4). The tumor uptake in the control group was

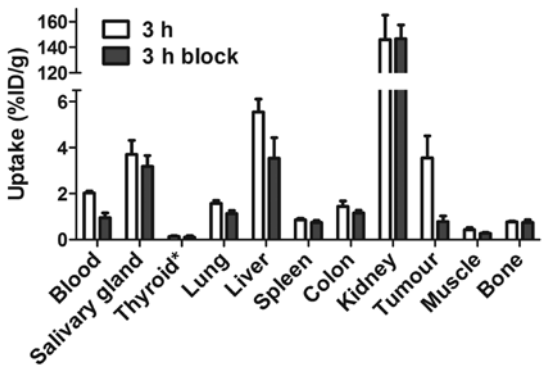

Figure 4. Specificity of ^{99m}Tc-ZEGFR:2377 uptake in A431 xenografts and EGFR-expressing organs in mice at 3 h after injection. In the blocked group, receptors were saturated by pre-injection of large excess of non-labeled anti-EGFR antibody cetuximab. The data are presented as average (n=4) and SD.

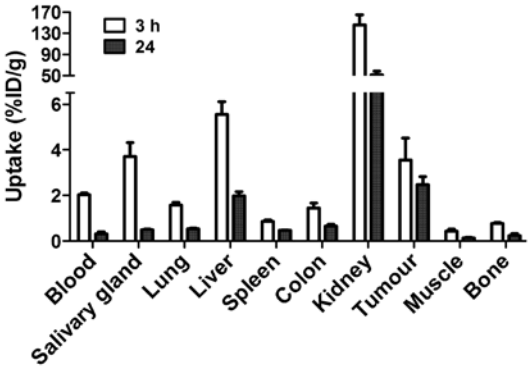

Figure 5. Biodistribution of ^{99m}Tc-ZEGFR:2377 in BALB/C nu/nu mice bearing EGFR-expressing A431 xenografts at 3 and 24 h after injection. The data are presented as average (n=4) and SD.

reduced 4.6-fold (P<0.005). Significant (P<0.05) reduction of radioactivity uptake in blood, liver, lung and muscle was also observed.

Fig. 5 shows the biodistribution of the ^{99m}Tc-ZEGFR:2377 conjugate at 3 and 24 h after injection in BALB/C nu/nu mice bearing EGFR-expressing A431 xenografts. The blood concentration was 2.03±0.08% ID/g at 3 h after injection, which suggests rather rapid blood clearance. The high uptake in kidneys (146±19% ID/g) indicates that the predominant excretion was via glomerular filtration followed by re-absorption which is typical for affibody molecules. Liver was the other organ with prominent uptake (5.6±0.6% ID/g), but excretion via the bile was minor. The gastrointestinal tracts with content contained only 4.0±0.5% of injected radioactivity. The tumor uptake (3.6±1% ID/g) exceeded the uptake in other organs and tissues except from liver, salivary glands and kidneys. However, the tumor-to-organ ratios (Fig. 6) were modest at this time-point. The tumor uptake had a tendency to decrease at 24 h, but the difference between tumor uptake values at 3 and 24 h was not significant (P=0.12). There was a highly significant (P<0.01) decrease of uptake in all other organs and tissues. This resulted in an appreciable increase of tumor-to-organ ratios at 24 h after injection (Fig. 6). This suggests that the preferable time-point for imaging would be at 24 h after injection.

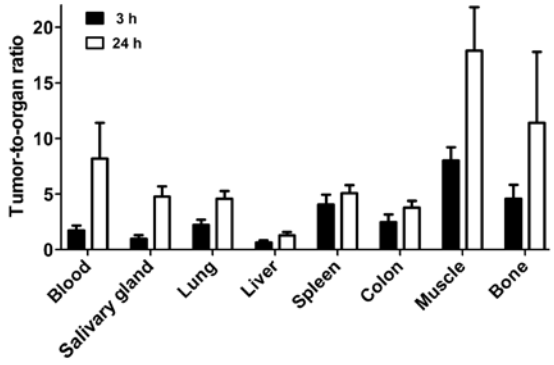

Figure 6. Tumor-to-organ ratios of ^{99m}Tc-ZEGFR:2377 in BALB/C nu/nu mice bearing EGFR-expressing A431 xenografts. The data are presented as average (n=4) and SD.

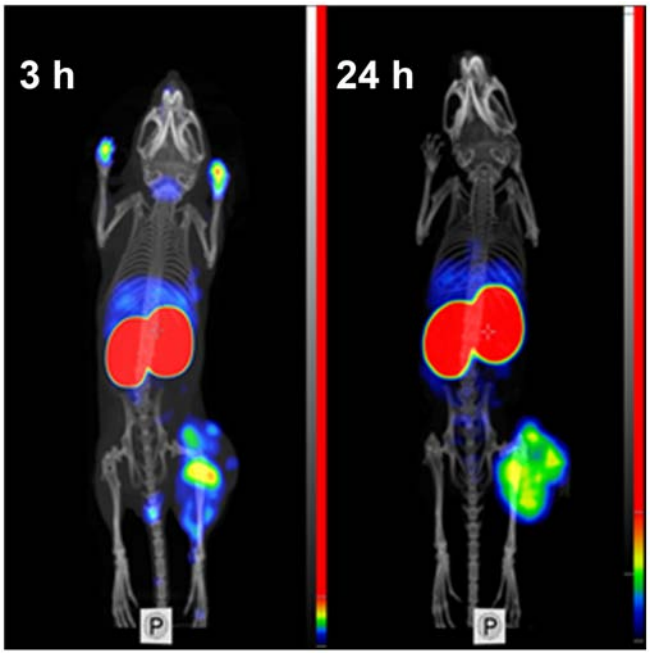

Figure 7. Imaging of EGFR-expressing A431 xenografts in BALB/C nu/nu mice using ^{99m}Tc-ZEGFR:2377 at 3 and 24 h after injection.

Feasibility of imaging of EGFR-expressing tumors using ^{99m}Tc-ZEGFR:2377 was demonstrated using microSPECT/CT (Fig. 7). Tumors on hind legs were clearly visualized. The irregular pattern of uptake reflected necrotic areas in the tumors. Radioactivity uptake in kidneys was considerably higher than in tumors. Other places with high radioactivity accumulation were liver and salivary gland (at 3 h after injection). At 3 h after injection, urinary bladder and, occasionally, urine contamination on front legs were also visualized. There was a reasonable contrast between tumors and other organs and tissues.

Discussion

Clinical studies have demonstrated that affibody molecules provide excellent sensitivity and specificity in imaging of HER2-expressing tumors using SPECT (47) and PET (33). Moreover, preclinical studies demonstrated feasibility of application of affibody molecules for imaging several molecular targets in cancer xenografts, e.g. EGFR (33), HER3 (48) IGF-1R (49), PDGFRβ (50) and CAIX (51). It would be attractive to apply our experience in development of HER2-imaging affibody molecule probes for development of probes to new targets. However, there are multiple amino-acid-alterations in the positions forming the target binding sites of new probes, which might influence both labeling chemistry and biodistribution pattern. The present study evaluated preconditions to labeling of affibody molecule-derived imaging probes using peptide-based cysteine-containing chelators. Chelators of that type provided a stable labeling of anti-HER2 affibody molecules with ^{99m}Tc and ^{188}Re (42,52). An apparent advantage of such chelators is that they are 'built in' in the recombinantly produced affibody molecule, and there is no need in additional steps of coupling of the chelator and purification of the conjugate. In addition, selection of amino acids in the chelator may enable a fine-tuning of residualizing properties of the label (52-54). However, there was a risk of losing site-specificity of the label when amino acid composition of an affibody molecules was modified (43). Indeed, the first experiments demonstrated release of over 30% of the ^{99m}Tc after dilution or under cysteine challenge (Table I). This might be an indication that some amino acids in ZEGFR:2377 form a chelating site, which competes with the cysteine-containing chelator, but has appreciably weaker complexing of the nuclide. To minimize the influence of such site, we introduced a cysteine challenge of the labeled conjugate before the final purification. We assumed that weakly bound nuclide would be stripped from the conjugate. The overall isolated yield has decreased to 69±1% in this case,

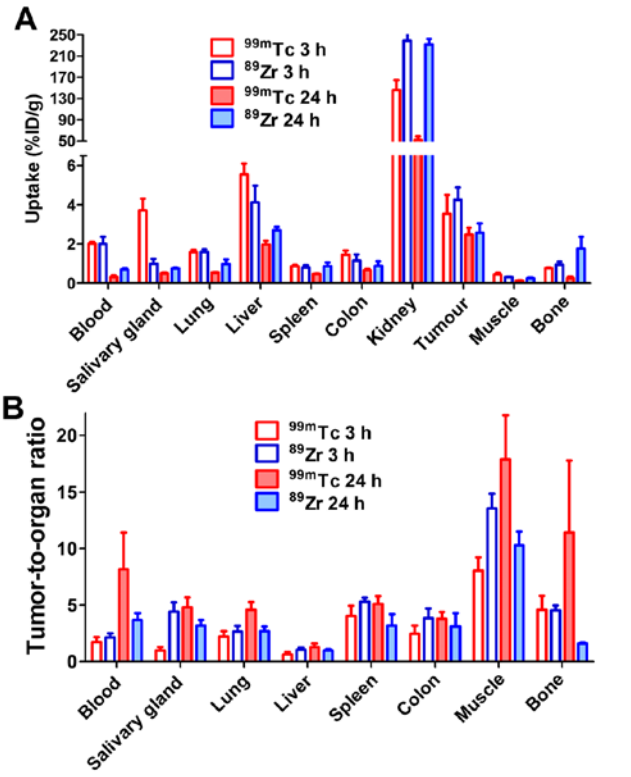

Figure 8. Comparison of biodistribution (A) and tumour-to-organ ratios (B) of ^{99m}Tc-ZEGFR:2377 and ^{89}Zr-ZEGFR:2377 in BALB/C nu/nu mice bearing A431 xenografts. Data for ^{89}Zr-ZEGFR:2377 are taken from (38).

but the conjugate could withstand the cysteine challenge (Table I). Adding an anti-oxidizing agent, sodium ascorbate, reduced the releases further, which indicates that re-oxidation of technetium is another, although minor, reason of release.

The ^{99m}Tc-ZEGFR:2377 retained capacity of specific binding to EGFR-expressing cells as it has been demonstrated by saturation of binding sites with both non-labeled ZEGFR:2377 and anti-EGFR antibody cetuximab (Fig. 2). Affinity of ^{99m}Tc-ZEGFR:2377 was 274±16 pM, in the same picomolar range as affinity of ^{89}Zr-labeled DFO-ZEGFR:2377 (160±60 pM) (38). The internalization by two EGFR-expressing cell lines was relatively slow (Fig. 3), which is typical for EGFR-binding affibody molecules (35,38). Blocking of EGFR receptors in A431 xenografts with the antibody cetuximab reduced significantly ($P<0.005$) uptake of ^{99m}Tc-ZEGFR:2377, which unambiguously demonstrated specificity of *in vivo* targeting (Fig. 4).

Recently, several approaches for radiofluorination of anti-EGFR affibody molecules have been reported (36,37). In similar tumor models (A431 xenografts), these tracers demonstrated tumor-to-blood ratios in the range from 1.5 to 2.4 at 3 h after injection. These values are similar to values provided by ^{99m}Tc-ZEGFR:2377 at this time-point (1.8±0.4). For comparison, the anti-HER2 ^{99m}Tc-ZHER2:2395 affibody molecule provided the tumor-to-blood ratio of 9±2 already 1 h after injection (42). The moderate values of tumor-to-blood ratios at early time-points (a few hours after injection) for anti-EGFR affibody molecules might be determined by two factors. First, there is an expression of EGFR in normal tissues, particularly in liver, and these tissues sequester part of the radiolabeled affibody molecules. Second, the affibody molecules are internalized quite slowly after binding to EGFR, i.e. remain reversibly bound to a cell surface. Thus, EGFR expressing tissues act as depots. Decrease of blood concentration of affibody molecules due to renal clearance shifts the equilibrium towards dissociation, and affibody molecules start to return to blood stream. Due to slower blood clearance, a good contrast might be obtained only several hours or at the next day after injection (35). This suggests that short-lived radionuclides, such as ^{18}F ($T_{1/2}$=109.8 min) or ^{68}Ga ($T_{1/2}$=67.6 min) are suboptimal for labeling of anti-EGFR affibody molecules. The longer half-life of ^{99m}Tc, 6.01 h, permits clinical imaging at several hours or even at the next day after injection (55,56). Due to absence of corpuscular radiation, more than 1100 MBq of ^{99m}Tc-labeled compounds might be injected resulting in low dose burden to the patient (57). This study demonstrated that tumor-to-organ ratios for ^{99m}Tc-ZEGFR:2377 increased appreciably at 24 h after injection compared to 3 h after injection. For example, the tumor-to-blood ratio increased 4.7-fold, and tumor-to-liver, tumor-to-lung, tumor-to-muscle and tumor-to-bone ratios increased 2-2.5-fold. This determines better contrast of imaging at later time-points and should provide better sensitivity of clinical imaging.

It has to be noted that the physical half-life of the label nuclide is only one of several factors determining contrast and feasibility of imaging. Chemical properties of a radionuclide and linker or chelators for its attachment to a tumor-targeting protein might influence the affinity, the cellular processing and retention of a radionuclide in tumor and normal tissues, its off-target interactions, and predominant excretion routes of a tracer and radiocatabolites (39). This might be exemplified by comparison of the biodistribution of ZEGFR:2377 labeled with ^{99m}Tc and with a long-lived ($T_{1/2}$=78.4 h) positron emitting radionuclide ^{89}Zr. We have recently studied ZEGFR:2377 labeled with ^{89}Zr using deferoxamine (DFO) chelator (38). Both studies used the same experimental methods and the same animal models, which facilitates comparison. The tumor uptake of both probes was similar at 3 and 24 h after injection (Fig. 8). At 3 h after injection, the uptake in normal organs and tissues was also quite similar; with exception that uptake of ^{99m}Tc is appreciably higher in salivary gland but lower in kidneys. At 24 h after injection, uptake of ^{99m}Tc is lower in all normal organ and tissues, which results in higher tumor-to-organ ratios compared to ^{89}Zr-ZEGFR:2377 (Fig. 8). Insight into why the differences occur might be gained by considering kidney retention. Affibody molecules are re-absorbed in proximal tubuli of kidneys and are rapidly internalized. Thus, the renal retention of a radionuclide depends on its residualizing properties. The renal uptake of ^{89}Zr is equal at 3 and 24 h, which suggests that this nuclide has strong residualizing properties. The renal uptake of ^{99m}Tc decreased ~3-fold at 24 h. This indicates that the residualizing properties of ^{99m}Tc label are moderate, and radiometabolites 'leak' from cells after internalization. It is likely that this is the reason why ^{99m}Tc clears more rapidly from other normal tissues.

^{99m}Tc-ZEGFR:2377 enabled good-contrast imaging of EGFR-expressing xenografts both at 3 and 24 h after injection (Fig. 7). The above suggests that the use of peptide-based cysteine-containing chelator at the C-terminus of ZEGFR:2377 affibody molecules for labeling with ^{99m}Tc is an adequate approach, providing a conjugate capable of visualization of EGFR expression in tumors. It would be attractive, of course, to find a labelling approach permitting a single-vial kit formulation, as for HER2-targeting affibody molecule (44). For ZEGFR:2377, a two-vial kit is possible, and a purification of the labeled is required. This complicates somewhat the labelling procedure. An evaluation of alternative approaches for ^{99m}Tc-labeling might be required before decision for clinical translation could be made.

In conclusion, the use of a peptide-based cysteine-containing chelator at the C-terminus provides labeling of the ZEGFR:2377 affibody molecule with ^{99m}Tc. However, an intermediate cysteine challenge is required to ensure that the nuclide is not complexed by a weak chelating site. Translation of previously gained knowledge to new affibody molecules is possible, but requires re-optimization of labeling chemistry since changes in amino acid composition might influence the site-specificity of labeling as well as the stability of the label.

Acknowledgements

The present study was supported by grants from the Swedish Research Council (Vetenskapsrådet) and the Swedish Cancer Society (Cancerfonden). The molecular imaging work in this publication has been supported by the Wallenberg infrastructure for PET-MRI (WIPPET), a Swedish nationally available imaging platform at Uppsala University, Sweden.

References

1. Kulkarni HR and Baum RP: Patient selection for personalized peptide receptor radionuclide therapy using Ga-68 somatostatin receptor PET/CT. PET Clin 9: 83-90, 2014.

2. Slobbe P, Poot AJ, Windhorst AD and van Dongen GA: PET imaging with small-molecule tyrosine kinase inhibitors: TKI-PET. Drug Discov Today 17: 1175-1187, 2012.
3. Altai M, Orlova A and Tolmachev V: Radiolabeled probes targeting tyrosine-kinase receptors for personalized medicine. Curr Pharm Des 20: 2275-2292, 2014.
4. Krause DS and Van Etten RA: Tyrosine kinases as targets for cancer therapy. N Engl J Med 353: 172-187, 2005.
5. Salomon DS, Brandt R, Ciardiello F and Normanno N: Epidermal growth factor-related peptides and their receptors in human malignancies. Crit Rev Oncol Hematol 19: 183-232, 1995.
6. Hedner C, Borg D, Nodin B, Karnevi E, Jirström K and Eberhard J: Expression and prognostic significance of human epidermal growth factor receptors 1 and 3 in gastric and esophageal adenocarcinoma. PLoS One 11: e0148101, 2016.
7. Ueda S, Ogata S, Tsuda H, Kawarabayashi N, Kimura M, Sugiura Y, Tamai S, Matsubara O, Hatsuse K and Mochizuki H: The correlation between cytoplasmic overexpression of epidermal growth factor receptor and tumor aggressiveness: Poor prognosis in patients with pancreatic ductal adenocarcinoma. Pancreas 29: e1-e8, 2004.
8. Growdon WB, Boisvert SL, Akhavanfard S, Oliva E, Dias-Santagata DC, Kojiro S, Horowitz NS, Iafrate AJ, Borger DR and Rueda BR: Decreased survival in EGFR gene amplified vulvar carcinoma. Gynecol Oncol 111: 289-297, 2008.
9. Young RJ, Rischin D, Fisher R, McArthur GA, Fox SB, Peters LJ, Corry J, Lim A, Waldeck K and Solomon B: Relationship between epidermal growth factor receptor status, $p16^{INK4A}$, and outcome in head and neck squamous cell carcinoma. Cancer Epidemiol Biomarkers Prev 20: 1230-1237, 2011.
10. Kros JM, Huizer K, Hernández-Laín A, Marucci G, Michotte A, Pollo B, Rushing EJ, Ribalta T, French P, Jaminé D, *et al*: Evidence-based diagnostic algorithm for glioma: Analysis of the results of Pathology Panel Review and Molecular Parameters of EORTC 26951 and 26882 Trials. J Clin Oncol 33: 1943-1950, 2015.
11. Roskoski R Jr: The ErbB/HER family of protein-tyrosine kinases and cancer. Pharmacol Res 79: 34-74, 2014.
12. Lynch TJ, Bell DW, Sordella R, Gurubhagavatula S, Okimoto RA, Brannigan BW, Harris PL, Haserlat SM, Supko JG, Haluska FG, *et al*: Activating mutations in the epidermal growth factor receptor underlying responsiveness of non-small-cell lung cancer to gefitinib. N Engl J Med 350: 2129-2139, 2004.
13. Paez JG, Jänne PA, Lee JC, Tracy S, Greulich H, Gabriel S, Herman P, Kaye FJ, Lindeman N, Boggon TJ, *et al*: EGFR mutations in lung cancer: Correlation with clinical response to gefitinib therapy. Science 304: 1497-1500, 2004.
14. Therkildsen C, Bergmann TK, Henrichsen-Schnack T, Ladelund S and Nilbert M: The predictive value of *KRAS*, *NRAS*, *BRAF*, *PIK3CA* and PTEN for anti-EGFR treatment in metastatic colorectal cancer: A systematic review and meta-analysis. Acta Oncol 53: 852-864, 2014.
15. Pirker R, Pereira JR, von Pawel J, Krzakowski M, Ramlau R, Park K, de Marinis F, Eberhardt WE, Paz-Ares L, Störkel S, *et al*: EGFR expression as a predictor of survival for first-line chemotherapy plus cetuximab in patients with advanced non-small-cell lung cancer: Analysis of data from the phase 3 FLEX study. Lancet Oncol 13: 33-42, 2012.
16. Cappuzzo F, Hirsch FR, Rossi E, Bartolini S, Ceresoli GL, Bemis L, Haney J, Witta S, Danenberg K, Domenichini I, *et al*: Epidermal growth factor receptor gene and protein and gefitinib sensitivity in non-small-cell lung cancer. J Natl Cancer Inst 97: 643-655, 2005.
17. Hirsch FR, Varella-Garcia M, Bunn PA Jr, Franklin WA, Dziadziuszko R, Thatcher N, Chang A, Parikh P, Pereira JR, Ciuleanu T, *et al*: Molecular predictors of outcome with gefitinib in a phase III placebo-controlled study in advanced non-small-cell lung cancer. J Clin Oncol 24: 5034-5042, 2006.
18. Bradley JD, Paulus R, Komaki R, Masters G, Blumenschein G, Schild S, Bogart J, Hu C, Forster K, Magliocco A, *et al*: Standard-dose versus high-dose conformal radiotherapy with concurrent and consolidation carboplatin plus paclitaxel with or without cetuximab for patients with stage IIIA or IIIB non-small-cell lung cancer (RTOG 0617): A randomised, two-by-two factorial phase 3 study. Lancet Oncol 16: 187-199, 2015.
19. Ang KK, Berkey BA, Tu X, Zhang HZ, Katz R, Hammond EH, Fu KK and Milas L: Impact of epidermal growth factor receptor expression on survival and pattern of relapse in patients with advanced head and neck carcinoma. Cancer Res 62: 7350-7356, 2002.
20. Bentzen SM, Atasoy BM, Daley FM, Dische S, Richman PI, Saunders MI, Trott KR and Wilson GD: Epidermal growth factor receptor expression in pretreatment biopsies from head and neck squamous cell carcinoma as a predictive factor for a benefit from accelerated radiation therapy in a randomized controlled trial. J Clin Oncol 23: 5560-5567, 2005.
21. Eriksen JG, Steiniche T and Overgaard J; Danish Head and Neck Cancer study group (DAHANCA): The influence of epidermal growth factor receptor and tumor differentiation on the response to accelerated radiotherapy of squamous cell carcinomas of the head and neck in the randomized DAHANCA 6 and 7 study. Radiother Oncol 74: 93-100, 2005.
22. Wang X, Niu H, Fan Q, Lu P, Ma C, Liu W, Liu Y, Li W, Hu S, Ling Y, *et al*: Predictive value of EGFR overexpression and gene amplification on icotinib efficacy in patients with advanced esophageal squamous cell carcinoma. Oncotarget 7: 24744-24751, 2016.
23. Humbert O, Riedinger JM, Charon-Barra C, Berriolo-Riedinger A, Desmoulins I, Lorgis V, Kanoun S, Coutant C, Fumoleau P, Cochet A, *et al*: Identification of biomarkers including ^{18}FDG-PET/CT for early prediction of response to neoadjuvant chemotherapy in triple negative breast cancer. Clin Cancer Res 21: 5460-5468, 2015.
24. Vignot S, Besse B, André F, Spano JP and Soria JC: Discrepancies between primary tumor and metastasis: A literature review on clinically established biomarkers. Crit Rev Oncol Hematol 84: 301-313, 2012.
25. Divgi CR, Welt S, Kris M, Real FX, Yeh SD, Gralla R, Merchant B, Schweighart S, Unger M, Larson SM, *et al*: Phase I and imaging trial of indium 111-labeled anti-epidermal growth factor receptor monoclonal antibody 225 in patients with squamous cell lung carcinoma. J Natl Cancer Inst 83: 97-104, 1991.
26. Cai W, Chen K, He L, Cao Q, Koong A and Chen X: Quantitative PET of EGFR expression in xenograft-bearing mice using ^{64}Cu-labeled cetuximab, a chimeric anti-EGFR monoclonal antibody. Eur J Nucl Med Mol Imaging 34: 850-858, 2007.
27. Nayak TK, Garmestani K, Milenic DE and Brechbiel MW: PET and MRI of metastatic peritoneal and pulmonary colorectal cancer in mice with human epidermal growth factor receptor 1-targeted ^{89}Zr-labeled panitumumab. J Nucl Med 53: 113-120, 2012.
28. Chang AJ, De Silva RA and Lapi SE: Development and characterization of ^{89}Zr-labeled panitumumab for immuno-positron emission tomographic imaging of the epidermal growth factor receptor. Mol Imaging 12: 17-27, 2013.
29. van Dijk LK, Hoeben BA, Kaanders JH, Franssen GM, Boerman OC and Bussink J: Imaging of epidermal growth factor receptor expression in head and neck cancer with SPECT/CT and ^{111}In-labeled cetuximab-F(ab')$_2$. J Nucl Med 54: 2118-2124, 2013.
30. van Dijk LK, Yim CB, Franssen GM, Kaanders JH, Rajander J, Solin O, Grönroos TJ, Boerman OC and Bussink J: PET of EGFR with ^{64}Cu-cetuximab-F(ab')$_2$ in mice with head and neck squamous cell carcinoma xenografts. Contrast Media Mol Imaging 11: 65-70, 2016.
31. Nygren PA and Skerra A: Binding proteins from alternative scaffolds. J Immunol Methods 290: 3-28, 2004.
32. Ahlgren S and Tolmachev V: Radionuclide molecular imaging using Affibody molecules. Curr Pharm Biotechnol 11: 581-589, 2010.
33. Sörensen J, Velikyan I, Sandberg D, Wennborg A, Feldwisch J, Tolmachev V, Orlova A, Sandström M, Lubberink M, Olofsson H, *et al*: Measuring HER2-receptor expression in metastatic breast cancer using [^{68}Ga]ABY-025 affibody PET/CT. Theranostics 6: 262-271, 2016.
34. Tolmachev V, Friedman M, Sandström M, Eriksson TL, Rosik D, Hodik M, Ståhl S, Frejd FY and Orlova A: Affibody molecules for epidermal growth factor receptor targeting in vivo: Aspects of dimerization and labeling chemistry. J Nucl Med 50: 274-283, 2009.
35. Tolmachev V, Rosik D, Wållberg H, Sjöberg A, Sandström M, Hansson M, Wennborg A and Orlova A: Imaging of EGFR expression in murine xenografts using site-specifically labelled anti-EGFR ^{111}In-DOTA-$Z_{EGFR:2377}$ affibody molecule: aspect of the injected tracer amount. Eur J Nucl Med Mol Imaging 37: 613-622, 2010.
36. Miao Z, Ren G, Liu H, Qi S, Wu S and Cheng Z: PET of EGFR expression with an ^{18}F-labeled affibody molecule. J Nucl Med 53: 1110-1118, 2012.

37. Su X, Cheng K, Jeon J, Shen B, Venturin GT, Hu X, Rao J, Chin FT, Wu H and Cheng Z: Comparison of two site-specifically ^{18}F-labeled affibodies for PET imaging of EGFR positive tumors. Mol Pharm 11: 3947-3956, 2014.
38. Garousi J, Andersson KG, Mitran B, Pichl ML, Ståhl S, Orlova A, Löfblom J and Tolmachev V: PET imaging of epidermal growth factor receptor expression in tumours using ^{89}Zr-labelled ZEGFR:2377 affibody molecules. Int J Oncol 48: 1325-1332, 2016.
39. Tolmachev V and Orlova A: Influence of labelling methods on biodistribution and imaging properties of radiolabelled peptides for visualisation of molecular therapeutic targets. Curr Med Chem 17: 2636-2655, 2010.
40. Slomka PJ, Pan T, Berman DS and Germano G: Advances in SPECT and PET Hardware. Prog Cardiovasc Dis 57: 566-578, 2015.
41. Banerjee SR, Maresca KP, Francesconi L, Valliant J, Babich JW and Zubieta J: New directions in the coordination chemistry of ^{99m}Tc: A reflection on technetium core structures and a strategy for new chelate design. Nucl Med Biol 32: 1-20, 2005.
42. Ahlgren S, Wållberg H, Tran TA, Widström C, Hjertman M, Abrahmsén L, Berndorff D, Dinkelborg LM, Cyr JE, Feldwisch J, *et al*: Targeting of HER2-expressing tumors with a site-specifically ^{99m}Tc-labeled recombinant affibody molecule, $Z_{HER2:2395}$, with C-terminally engineered cysteine. J Nucl Med 50: 781-789, 2009.
43. Lindberg H, Hofström C, Altai M, Honorvar H, Wållberg H, Orlova A, Ståhl S, Gräslund T and Tolmachev V: Evaluation of a HER2-targeting affibody molecule combining an N-terminal HEHEHE-tag with a GGGC chelator for ^{99m}Tc-labelling at the C terminus. Tumour Biol 33: 641-651, 2012.
44. Ahlgren S, Andersson K and Tolmachev V: Kit formulation for ^{99m}Tc-labeling of recombinant anti-HER2 affibody molecules with a C-terminally engineered cysteine. Nucl Med Biol 37: 539-546, 2010.
45. Hnatowich DJ, Virzi F, Fogarasi M, Rusckowski M and Winnard P Jr: Can a cysteine challenge assay predict the in vivo behavior of ^{99m}Tc-labeled antibodies? Nucl Med Biol 21: 1035-1044, 1994.
46. Wållberg H and Orlova A: Slow internalization of anti-HER2 synthetic affibody monomer ^{111}In-DOTA-$Z_{HER2:342-pep2}$: implications for development of labeled tracers. Cancer Biother Radiopharm 23: 435-442, 2008.
47. Sörensen J, Sandberg D, Sandström M, Wennborg A, Feldwisch J, Tolmachev V, Åström G, Lubberink M, Garske-Román U, Carlsson J, *et al*: First-in-human molecular imaging of HER2 expression in breast cancer metastases using the ^{111}In-ABY-025 affibody molecule. J Nucl Med 55: 730-735, 2014.
48. Andersson KG, Rosestedt M, Varasteh Z, Malm M, Sandström M, Tolmachev V, Löfblom J, Ståhl S and Orlova A: Comparative evaluation of ^{111}In-labeled NOTA-conjugated affibody molecules for visualization of HER3 expression in malignant tumors. Oncol Rep 34: 1042-1048, 2015.
49. Mitran B, Altai M, Hofström C, Honarvar H, Sandström M, Orlova A, Tolmachev V and Gräslund T: Evaluation of ^{99m}Tc-$Z_{IGF1R:4551}$-GGGC affibody molecule, a new probe for imaging of insulin-like growth factor type 1 receptor expression. Amino Acids 47: 303-315, 2015.
50. Tolmachev V, Varasteh Z, Honarvar H, Hosseinimehr SJ, Eriksson O, Jonasson P, Frejd FY, Abrahmsen L and Orlova A: Imaging of platelet-derived growth factor receptor β expression in glioblastoma xenografts using affibody molecule ^{111}In-DOTA-Z09591. J Nucl Med 55: 294-300, 2014.
51. Honarvar H, Garousi J, Gunneriusson E, Höidén-Guthenberg I, Altai M, Widström C, Tolmachev V and Frejd FY: Imaging of CAIX-expressing xenografts *in vivo* using ^{99m}Tc-HEHEHE-ZCAIX:1 affibody molecule. Int J Oncol 46: 513-520, 2015.
52. Altai M, Honarvar H, Wållberg H, Strand J, Varasteh Z, Rosestedt M, Orlova A, Dunås F, Sandström M, Löfblom J, *et al*: Selection of an optimal cysteine-containing peptide-based chelator for labeling of affibody molecules with ^{188}Re. Eur J Med Chem 87: 519-528, 2014.
53. Wållberg H, Orlova A, Altai M, Hosseinimehr SJ, Widström C, Malmberg J, Ståhl S and Tolmachev V: Molecular design and optimization of ^{99m}Tc-labeled recombinant affibody molecules improves their biodistribution and imaging properties. J Nucl Med 52: 461-469, 2011.
54. Altai M, Wållberg H, Orlova A, Rosestedt M, Hosseinimehr SJ, Tolmachev V and Ståhl S: Order of amino acids in C-terminal cysteine-containing peptide-based chelators influences cellular processing and biodistribution of ^{99m}Tc-labeled recombinant Affibody molecules. Amino Acid 42: 1975-1985, 2012.
55. Moffat FL Jr, Pinsky CM, Hammershaimb L, Petrelli NJ, Patt YZ, Whaley FS and Goldenberg DM; The Immunomedics Study Group: Clinical utility of external immunoscintigraphy with the IMMU-4 technetium-99m Fab' antibody fragment in patients undergoing surgery for carcinoma of the colon and rectum: Results of a pivotal, phase III trial. J Clin Oncol 14: 2295-2305, 1996.
56. Serafini AN, Klein JL, Wolff BG, Baum R, Chetanneau A, Pecking A, Fischman AJ, Hoover HC Jr, Wynant GE, Subramanian R, *et al*: Radioimmunoscintigraphy of recurrent, metastatic, or occult colorectal cancer with technetium 99m-labeled totally human monoclonal antibody 88BV59: Results of pivotal, phase III multicenter studies. J Clin Oncol 16: 1777-1787, 1998.
57. Schwochau K: Technetium radiopharmaceuticals: Fundamentals, synthesis, structure and development. Angew Chem Int Ed Engl 33: 2258-2267, 1994.